Journal of Molecular Liquids 368 (2022) 120781

Contents lists available at ScienceDirect

Journal of Molecular Liquids

journal homepage: www.elsevier.com/locate/molliq

Novel biomimetic nanocomposite for investigation of drug metabolism

Diána Balogh-Weiser [a,b,*], László Poppe [a,c,d,*], Balázs Kenéz [a], Balázs Decsi [a], Gábor Koplányi [a], Gábor Katona [e], Benjámin Gyarmati [b], Ferenc Ender [f,g], György T. Balogh [h,i,*]

[a] Department of Organic Chemistry and Technology, Faculty of Chemical Technology and Biotechnology, Budapest University of Technology and Economics, Műegyetem rkp. 3. H-1111, Budapest, Hungary
[b] Department of Physical Chemistry and Materials Science, Faculty of Chemical Technology and Biotechnology, Budapest University of Technology and Economics, Műegyetem rkp. 3. H-1111, Budapest, Hungary
[c] Biocatalysis and Biotransformation Research Centre, Faculty of Chemistry and Chemical Engineering, Babes-Bolyai University of Cluj-Napoca, Arany János Str. 11, RO-400028 Cluj-Napoca, Romania
[d] Institute of Pharmaceutical Technology and Regulatory Affairs Faculty of Pharmacy, University of Szeged, Eötvös u. 6, H-6720 Szeged, Hungary
[e] Institute of Pharmaceutical Technology and Regulatory Affairs Faculty of Pharmacy, University of Szeged, Eötvös u. 6, H-6720 Szeged, Hungary
[f] Spinsplit LLC., Vend u. 17. H-1025, Budapest, Hungary
[g] Department of Electron Devices, Faculty of Electrical Engineering and Informatics, Budapest University of Technology and Economics, Műegyetem rkp. 3. H-1111, Budapest, Hungary
[h] Department of Chemical and Environmental Process Engineering Faculty of Chemical Technology and Biotechnology, Budapest University of Technology and Economics, Műegyetem rkp. 3. H-1111, Budapest, Hungary
[i] Institute of Pharmacodynamics and Biopharmacy Faculty of Pharmacy, University of Szeged Eötvös u. 6, H-6720 Szeged, Hungary

ARTICLE INFO

Article history:
Received 16 September 2022
Revised 5 November 2022
Accepted 8 November 2022
Available online 12 November 2022

ABSTRACT

In vitro mimicking of hepatic drug metabolism is a key issue in early-stage drug discovery. Synthetic metalloporphyrins show structural similarity with the heme type prosthetic group of cytochrome P450 as primary hepatic enzyme in oxidative drug biotransformation. Therefore, they can catalyze these oxidations. Concerning economical aspects and the poor stability of metalloporphyrin, their immobilization onto or into solid carriers can be promising solution. This study presents a novel immobilized metalloporphyrin nanocomposite system and its potential use as biomimetic catalysts. The developed two-step immobilization procedure consists of two main steps. First, the ionic binding of *meso*-tetra (parasulphonatophenyl) iron porphyrin onto functionalized magnetic nanoparticles is established, followed by embedding the nanoparticles into polylactic acid nanofibers by electrospinning technique. Due to the synergistic morphological and chemo-structural advantages of binding onto nanoparticles and embedding in polymeric matrices the biomimetic efficiency of metalloporphyrin can be remarkably enhanced, while substrate conversion value was tenfold larger than which could be achieved with classic human liver microsomal system.

© 2022 The Author(s). Published by Elsevier B.V. This is an open access article under the CC BY-NC-ND license (http://creativecommons.org/licenses/by-nc-nd/4.0/).

1. Introduction

The cytochrome P450 (CyP450)-dependent oxidative metabolism of endogenous molecules and xenobiotics aroused a great interest in the last few decades. [1] In the living body, the metabolism of a drug molecule is usually initiated by an oxidative transformation catalyzed by a member of the CyP450 enzyme superfamily. Therefore, the metabolic stability of a drug molecule against CyP450 related oxidative biotransformation is an important factor to be considered during the drug development process. [2] Liver microsomes contain CyP enzymes in high concentrations. Therefore, microsome-based in vitro methods are often used to identify oxidative metabolites of drug candidate molecules. [3] The identification of the major oxidative metabolites provides useful information for optimizing the structure of drug candidate molecules. However, there are certain limitations associated with using biological systems. The substrate molecule can be used in low concentrations only; hence the metabolites are available in small quantities. A complex biological matrix is present in the reaction medium which can react with or adsorb the formed metabolites. Therefore, analysis of the samples and the isolation of the products found to be difficult. [4] Biomimetic systems may provide a promising alternative approach to address the disadvan-

* Corresponding authors at: Department of Organic Chemistry and Technology, Faculty of Chemical Technology and Biotechnology, Budapest University of Technology and Economics, Műegyetem rkp. 3. H-1111, Budapest, Hungary (D. Balogh-Weiser, L. Poppe). Department of Chemical and Environmental Process Engineering Faculty of Chemical Technology and Biotechnology, Budapest University of Technology and Economics, Műegyetem rkp. 3. H-1111, Budapest, Hungary (G.T. Balogh).

E-mail addresses: balogh.weiser.diana@vbk.bme.hu (D. Balogh-Weiser), poppe.laszlo@vbk.bme.hu (L. Poppe), balogh.gyorgy@vbk.bme.hu (G.T. Balogh).

https://doi.org/10.1016/j.molliq.2022.120781
0167-7322/© 2022 The Author(s). Published by Elsevier B.V.
This is an open access article under the CC BY-NC-ND license (http://creativecommons.org/licenses/by-nc-nd/4.0/).

tages of the biological models. Biomimetic systems imitate the catalytic behavior of the CyP enzymes; therefore, they generate metabolites from the parent molecule in one step, yet the complex biological matrix is not required. Such system can be developed by using of synthetic metalloporphyrins as biomimetic catalysts. The application of metalloporphyrins is based on their structural similarities to the protoporphyrin-IX moiety, found in the prosthetic heme group at the active site of the CyP enzymes. [5–7] On the one hand this functional similarity makes metalloporphyrins a promising approach to generate metabolites. On the other hand, metalloporphyrins suffer from relatively low stability in homogeneous oxidative systems and the recovery of the catalysts is challenging. [8].

We propose the immobilization of such molecules onto or into solid support to overcome the above limitations. [9] Several supports, such as modified irregular silica gels [10], magnetic nanoparticles [11], kaolinite [12] and carbon nanotubes [13] have been previously used for metalloporphyrin immobilization. The stability of the immobilized porphyrin catalysts can be improved significantly and their separation from the reaction media can be achieved by a simple filtration or by magnetic force (in case of magnetic material). For entrapment or embedding of porphyrins in a non-solvable matrix can be applied such as zeolites [14], polymer matrix [15] and alumina [16].

Advances in material science and nanotechnology in the recent decades enabled the formation of nanoscale materials. By taking the advantages of down-scaling, the resulted materials may show better properties than non-nanostructured systems. [17] Nanofiber based products represent a wide group of such novel products used widely both in the industry and in research. Nanofibers can be applied as filter media [18], reinforcement in composites, [19] etc. One important application of nanofibers is the entrapment of a desired substance. Therefore, nanofibers were also found to be excellent carriers. Such examples are bioactive agents (small drug molecules or therapeutic macromolecules) [20], inorganic [21], or (bio)organic [22] catalysts for heterogeneous catalysis. The formation of nanofibrous composites is one of the promising applications of nanofibers. Such composites may improve the physical properties of pure nanofibers (cellulose nanoparticles in polyvinyl alcohol) [23], they can be used as a chemical sensor (metal salts in polyaniline) [24]. They were also used to improve catalytic properties by entrapping of sensitive [25] or expensive catalyst [26] yet providing catalyst reusability and eliminating catalyst loss. Usually, nanoparticles are added to the precursor which results in composite nanofibers upon fiber formation. Electrospinning is a widely available technique to produce nanofibers and nanofibrous composites. During electrospinning the polymer precursor (polymer solution or melt with or without nanoparticles) is lead and distributed into a single (or multiple) high surface to volume ratio droplet, which is subjected to high electric field gradient. The electric field causes charge re-distribution in the precursor droplet which results in strong repulsion between the charges and an elongated jet is formed. Once the jet is stabilized, fiber formation starts with a whipping motion towards the grounded collector, simultaneously losing the solvent content or cooling down and solidifying rapidly, resulting in a solid nanofibrous net with typically micron to submicron diameter uniform fibers [27].

There are some studies about the combination of magnetic nanoparticles and nanofibrous materials, based on the in-situ formation of particles on the fibers or the entrapment of prepared particles inside the fibers. These composite materials were utilized in versatile applications such as photodegradation, magnetic materials, tissue engineering, wastewater treatment or magnetic hyperthermia. [28–32].

The aim of this research was to develop a nanostructured composite material as solid carrier of a biomimetic catalyst, in which components could have positive synergism for the chemical and mechanical stability and activity of the catalyst. The goal was to select two type of nanocarriers, one of which is able to rapid and capacitive immobilization of metalloporphyrin and has good dispersibility, and other one, which could create a protective and easy-to-handle "package" with good permeability. Thus, by combining magnetic nanoparticles with polylactic acid (PLA) nanofibers a novel composite material was produced, while as an efficient carrier for sensitive metalloporphyrins. During a so-called 2nd generation immobilization method, first *meso*-tetra (parasulphonatophenyl) iron porphyrin (FeTPPS) was bounded to amino-functionalized magnetic nanoparticles (MNPs) via ionic interactions, then the FeTPPS-MNPs catalysts were embedded into PLA nanofibers using solvent electrospinning technique (Fig. 1.). Since such systems was not described previously, this work reports the preparation and optimization of a novel porphyrin based nanofibrous composite catalysts system. The biomimetic ability of the nanocomposites was also investigated on the calcium channel blocker amlodipine as a model drug compound. Although composites of PLA nanofibers and MNPs, mainly applied as drug delivery systems had been reported in few cases, MNP/PLA nanocomposites have been never applied as biomimetic catalytic system. [33,34].

2. Materials and methods

2.1. Production of FeTPPS-MNP/PLA nanocomposite

Polylactic acid (PLA, 0.8 g) and mixture of dichloromethane (DCM) and *N*,*N*-dimethyl-formamide (DMF) (6:1 V/V, 9.2 g) were added into a 20 mL vial then the mixture was shaken until the PLA was completely dissolved. The corresponding amount of FeTPPS-MNP suspension was added to the PLA solution then the mixture was intensely shaken finally sonicated (10 min, RT, with full power at 45 kHz, Emmi 20HC ultrasonic bath, Emag AG, Mörfelden-Walldorf, Germany). The prepared precursor mixture was loaded into a syringe and was driven through a laboratory electrospinning machine (Spincube, Spinsplit Llc, Budapest, Hungary). The vertical electrospinning system was operated with flow-rate 45 μL min^{-1}, an 18 Gauge emitter, 21 kV electric field, the distance between the emitter and collector was 10 cm, and the sample was collected on aluminum foil placed onto the plane collector (Fig. 2). Nanocomposite was removed from aluminum foil then dried until vacuum (2 h, 100 mbar, Binder VDL 23 vacuum drying chamber, Binder GmbH, Tuttlingen, Germany).

2.2. Biomimetic oxidation catalyzed by FeTPPS-MNP/PLA nanocomposite

In Eppendorf tubes 10.0 mg of FeTPPS-MNP/PLA nanocomposite and 335 μL amlodipine solution (2.5 mg mL^{-1} in the mixture of methanol and acetate buffer (4:1 V/V, pH = 4.5, 64 mM)) were added and homogenized by shaking (at 800 rpm, 25 °C, Vibramax 100, Heidolph NA Llc, Schwabach, Germany). The reaction mixture was diluted to 1.0 mL with the solvent mixture then the reaction was started with the addition of *t*-BuOOH solution (1 μL, 5 equivalents to amlodipine (**1**), 70 % aqueous solution). The tubes were then shaken for 10 min (at 1200 rpm, 25 °C Vibramax 100, Heidolph NA Llc, Schwabach, Germany) then 75 μL of sample was taken from each tube. The samples were diluted to 2.0 mL with methanol and analyzed by UV–vis spectrophotometer (Genesys-2, Thermo Fisher Scientific Inc., Waltham, MA, USA) recording full spectra from 200 to 700 nm. Conversion value (*c*) of the biomimetic reactions was calculated by the characteristic adsorption of

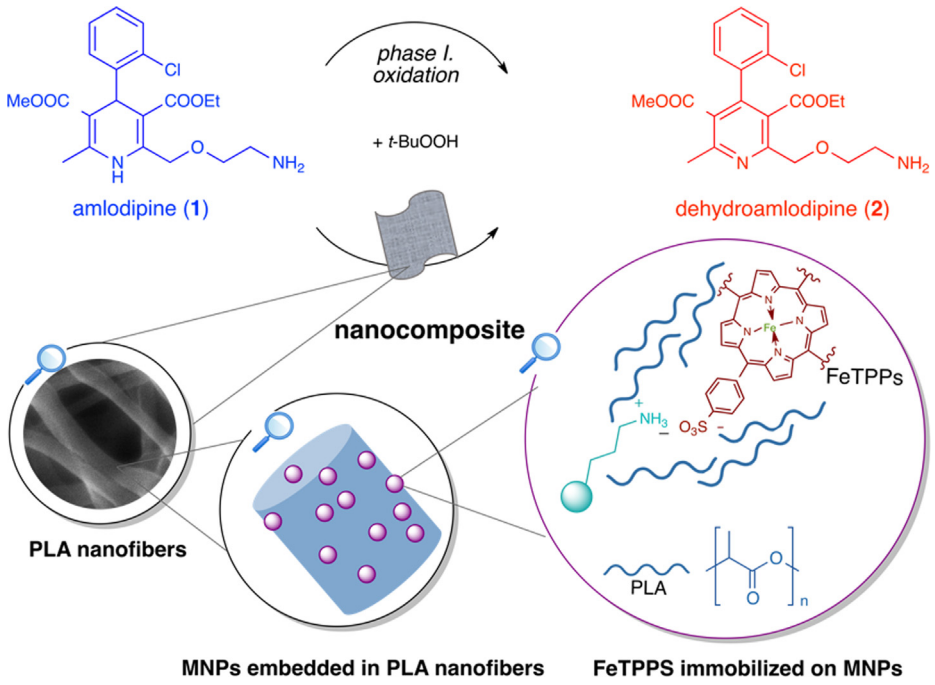

Fig. 1. Scheme of biomimetic oxidation of amlodipine (**1**) and its human major metabolite dehydroamlodipine (**2**) catalyzed by a nanocomposite catalyst consisting of immobilized FeTPPS on MNPs embedded within PLA nanofibers.

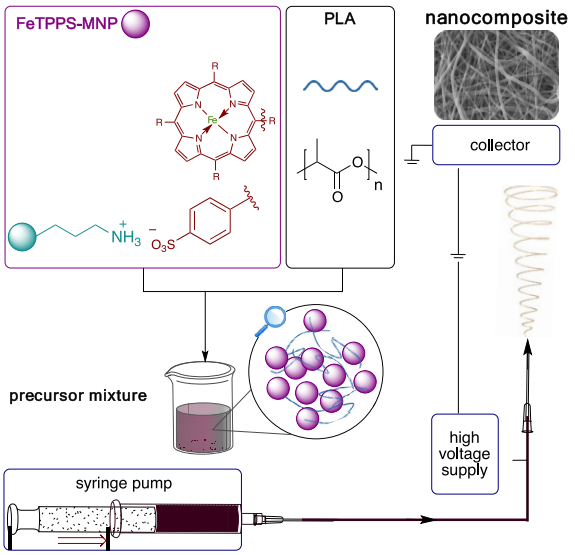

Fig. 2. The scheme of precursor preparation and electrospinning process for the nanocomposite FeTPPS catalysts.

Amlodipine (**1**) λ = 360 nm. The product profile of biomimetic reaction was investigated by LC-MS (see in ESI Section 2.11).

2.3. Calculations

The efficiency of catalyst immobilization is defined with immobilization yield (Y_I, shows the immobilized proportion of initial catalyst amount):

$$Y_I[\%] = 1 - \left(\frac{C_{2P}}{C_{1P}}\right) \times 100$$

where C_{1P} is the initial metalloporphyrin concentration, C_{2P} is the residual metalloporphyrin concentration in the binding solution.

The catalytic parameters such as conversion (c), biomimetic activity (UB, which shows the converted substrate amount per unit of time and total mass of immobilized catalyst) and specific biomimetic activity (UP, which shows the converted substrate amount per unit of time and total amount of metalloporphyrin catalyst) and turn over number (TON, which shows the amount of converted substrate to product per amount of catalytic molecule) were determined by the following equations:

$$\boldsymbol{c}[\%] = \left(1 - \frac{\boldsymbol{C_R}}{\boldsymbol{C_S}}\right) \times 100$$

where C_S is the concentration of the initial substrate and C_R is the concentration of the residual substrate based on the absorbance at λ = 360 nm and the calibration curve,

$$\boldsymbol{U_B}\left[\boldsymbol{Ug^{-1}}\right] = \frac{\boldsymbol{n_{s0}} \times \boldsymbol{c}}{\boldsymbol{t} \times \boldsymbol{m_B}}$$

where n_{S0} is the initial amount of the substrate, c is conversion, t is reaction time in min, m_B is the mass of the biomimetic catalyst in g,

$$\boldsymbol{U_P}\left[\boldsymbol{Ug^{-1}}\right] = \frac{\boldsymbol{n_{s0}} \times \boldsymbol{c}}{\boldsymbol{t} \times \boldsymbol{m_P}}$$

where m_P is the mass of the metalloporphyrin in g in the immobilized biomimetic catalyst,

$$\boldsymbol{TON}[-] = \frac{\boldsymbol{n_P}}{\boldsymbol{n_{cat}}}$$

where n_P is the amount of product in μmol and n_{cat} is the amount of the metalloporphyrin in μmol in the immobilized biomimetic catalyst.

Other details related to Experimental session can be found in the electronic supplementary information document (ESI.).

3. Results and discussion

3.1. 1st generation immobilization of metalloporphyrin

In the first part of the study, simple immobilization of FeTPPS metalloporphyrin onto magnetic nanoparticles and into PLA nanofibers were performed. Because immobilization capacity and catalysts leaching are generally critical points of immobilized systems, the binding capacity of the supports and the release of FeTPPS were examined by the specific detection of FeTPPS by UV–vis spectrophotometry (see in ESI FigS1). The results showed that the immobilization yield (Y_I, %) was more than 99 % in case of ionic binding of FeTPPS onto MNPs and the simple entrapment of FeTPPS molecules into PLA nanofibers (see in ESI Table S1, panel A). Since no metalloporphyrin could be detected in the washing buffer of MNPs after FeTPPS binding, the nanoparticles could immobilize FeTPPS strong enough to avoid leaching. In contrast, PLA nanofibers could not retain sufficiently the small FeTPPS molecules, because more than 90 % of the entrapped FeTPPS was washed out (see in ESI, Table S1, panel B.). Our previous studies indicated that functionalized magnetic nanoparticles are promising carriers for small-sized catalysts such as metalloporphyrins as well as for large molecules like enzymes. [11,22,35–37] However, aggregation of the nanoparticles partially due to the required magnetic forces for their separation could cause difficulties such as reduction in catalytic activity. Embedding or cross-linking of nanoparticles can eliminate these problems. [38,39] Our results and experiences indicate how a 2nd generation immobilization procedure involving fast and efficient ionic binding with MNPs and the good entrapment ability and stability of PLA nanofibers can diminish these problems.

3.2. 2nd generation immobilization of metalloporphyrin

During the combined immobilization process, the rapid ionic binding of FeTPPS on the amino-functionalized MNPs was performed, then the suspension of the metalloporphyrin loaded particles at different amount were mixed with the PLA solution. Finally, the precursor mixture was introduced to a laboratory electrospinning equipment and the prepared fibrous nanocomposite material was collected on a plate collector (Fig. 2.).

The MNP/PLA ratio in the precursor mixture was systematically changed according to seven different dry mass ratios of FeTPPS-MNPs/PLA (5, 2.5, 1.25, 0.63, 0.31, 0.16 and 0 w/w% FeTPPS-MNPs in dry FeTPPS-MNPs/PLA nanocomposite). The FeTPPS-MNPs content of the fibrous composite is a key parameter because it directly affects the catalytic activity, as well as the viscosity of the precursor. Nanofiber yield of the electrospinning process also depends on the precursor viscosity, therefore the viscosity and spinnability of the precursor containing different amounts of nanoparticles were investigated (Table 1). Apart from the highest MNP content (5 w/w% FeTPPS-MNP), the presence of magnetic nanoparticles caused negligible changes in viscosity values. The quantitative description of the electrospinning process in terms of successful fiber production is often challenging and not yet standardized. To overcome this issue, we proposed to use the spinnability score (S) in our previous study to evaluate the fiber fabrication process. [22] In general, the presence of magnetic nanoparticles influenced the electrospinning process positively at 0.31–2.5 w/w% of FeTPPS-MNPs in FeTPPS-MNP/PLA mixture, while better Spinnability score could be achieved by the applying of them in the precursor system (Table 1.). The morphology of the final fibrous product is also important. Uniform fibers are favorable without heterogeneities (beads, confluences etc.). The nanofibrous matrices were investigated by scanning electron microscope (SEM), SEM images were evaluated by an image analyzer software to determine fiber diameters. The analysis indicates that the thickness of the nanofibers was increased compared to the MNP-FeTPPS free PLA fibers in every case (Table 1 and Fig. 2.). It can be said that the higher the MNP-FeTPPS content, the thicker the nanofiber is but under 1.25 % MNP-FeTPPS content, the average diameter is close to constant.

Table 1
Effect of FeTPPS-MNPs content on the viscosity, spinnability of precursor mixture and fiber diameter of the nanocomposite.

FeTPPS-MNPs content[a]	Viscosity [mPas]	S [b] [-]	Fiber diameter [nm]
5	855 ± 156	1	1224 ± 310
2.5	496 ± 22	2	900 ± 296
1.25	590 ± 106	2	788 ± 156
0.63	501 ± 98	3	842 ± 207
0.31	432 ± 38	2	812 ± 177
0.16	553 ± 64	1	788 ± 186
0	525 ± 37	1	606 ± 184

[a] content of FeTPPS-MNP in dry FeTPPS-MNP/PLA nanocomposite; [b] S: Spinnability score is given according to the following consideration: 0 (no fiber formation), 1 (very limited fiber formation, unstable jet), 2 (non-continuous fiber formation with weak to moderate yield), 3 (continuous fiber formation with stable jet and high yield.

Morphological investigation showed that every composite including MNPs had relatively uniform fibrous structure. Probably, MNPs with diameter 250 ± 10 nm (Fig. 3a) could be well dispersed in PLA fibers, while the morphology of empty PLA fibers (without MNPs) was similar to MNPs containing composite PLA materials (Fig. 3b–h). At the highest nanoparticle content (5 w/w% FeTPPS-MNP) some heterogeneities (beads and/or aggregates) could be found (Fig. 3h). Elemental analysis of nanocomposites was also performed applying a SEM coupled Energy Dispersive X-ray Analysis (SEM-EDAX).

Table 2 presents atomic % of the four relevant elements (C, O, Si and Fe) in nanocomposites with different FeTPPS-MNP content, where Si and Fe are obviously specific for silica shell and iron oxide core of MNPs. The results showed that as the MNP content increases, the Si and Fe contents were also increased respectively.

The distribution of FeTPPS-MNPs in fiber mats was investigated by constructing Raman chemical maps. To ensure smooth and even surface to eliminate focusing errors of samples, during analysis the sample holder glass slide was covered with a slice of aluminum foil containing electrospun nanofibers and placed under the Raman microscope. Further advantage of the application aluminum foil was the low spectral background and lack of spectral features, which may interfere with the measurement. To achieve well distinguishable spectral difference between the poor Raman scatterer Fe_3O_4-based FeTPPS-MNPs and PLA, laser irradiation induced phase transformation was applied. Relative high laser exposure (6 mW) of the magnetite nanoparticles tends to cause the oxidation of Fe_3O_4 into stable α-Fe_2O_3 via metastable γ-Fe_2O_3. [40] In the Raman spectra obtained after exposure peaks were observed at 602, 493, 401, 286, 240 and 220 cm^{-1} corresponding to the vibration modes of Fe-O bonds, of which the bands at 286 and 220 cm^{-1} are due to the oxidation reaction occurred during Raman experiment, indicating successful α-Fe_2O_3 forming resulting in sharp spectral differences of FeTPPS-MNPs in comparison to PLA [41]. The 1303 cm^{-1} broad band is attributed to the second order scattering of hematite. The characteristic peaks at 602, 493 and 220 cm^{-1} showing no overlap with the corresponding spectral region of PLA were selected for further profiling (Figure S2). After structural examination of laser treated PLA and FeTPPS-MNP, Raman mapping was carried out to investigate the distribution of FeTPPS-MNPs in the different nanofibers. The profiled Raman

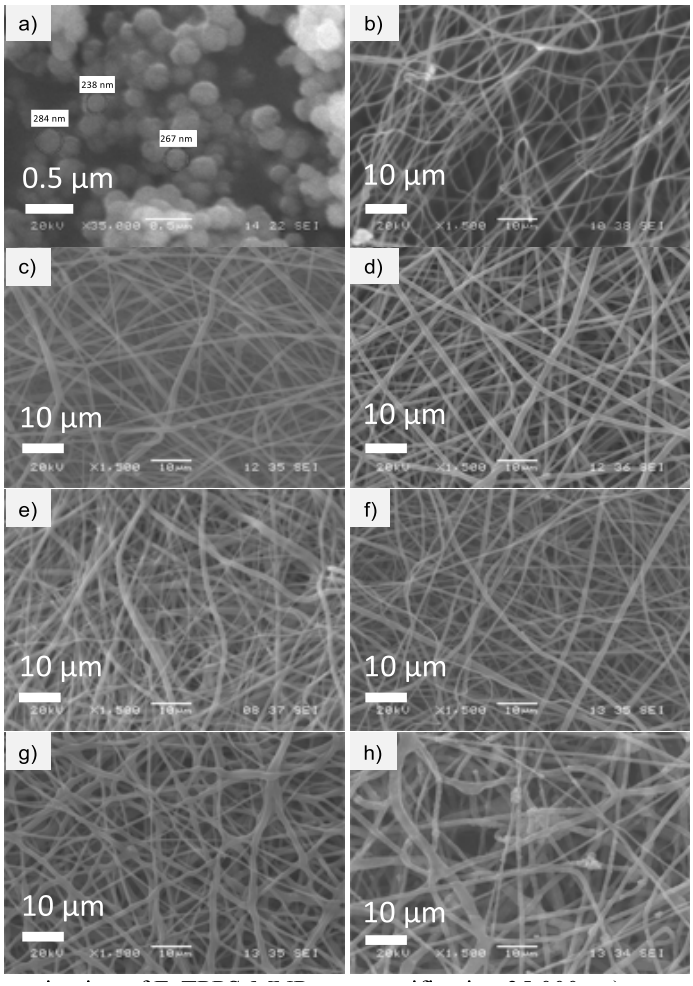

Fig. 3. Morphological investigation of FeTPPS-MNPs at magnification 35,000 × a) empty PLA nanofibers b) and c) - h) PLA nanocomposites loaded with FeTPPS-MNP content of 0.16 w/w%, 0.31 w/w%, 0.63 w/w%, 1.25 w/w%, 2.5 w/w%, and 5 w/w%, at magnification 1,500 × respectively.

Table 2
Elemental analysis of FeTPPS-MNP/PLA nanocomposites.

FeTPPS-MNPs content[a]	*Atomic %*			
	C	O	Si	Fe
5	72.6 ± 1.19	23.4 ± 1.19	0.47 ± 0.04	3.46 ± 0.53
2.5	83.8 ± 2.4	13.4 ± 1.42	0.24 ± 0.11	2.50 ± 1.66
1.25	80.9 ± 2.74	18.0 ± 2.74	0.13 ± 0.10	0.98 ± 0.01
0.63	77.6 ± 1.96	21.8 ± 1.98	0.13 ± 0.04	0.46 ± 0.15
0.31	70.5 ± 0.52	29.2 ± 0.55	0.07 ± 0.01	0.26 ± 0.04
0.16	75.7 ± 3.24	24.1 ± 3.09	0.04 ± 0.01	0.03 ± 0.02
0	85.2 ± 1.23	14.8 ± 1.22	0.02 ± 0.01	< 0.01

chemical maps of fiber mats containing different amount of FeTPPS-MNPs were normalized to frequency of occurrence of selected spectral region (Fig. 4). The different colors of the chemical map indicate the relative intensity change of FeTPPS-MNP content in the nanofibers. Red color indicates its strong existence, the green area shows a mixed composition, whereas blue color marks those regions of the map, whose spectral resolution contains different spectra, characteristic rather for PLA. The relative intensity changes are in accordance with different FeTPPS-MNP content. Accordingly, the more intensively red regions of chemical map verified the increased extent of FeTPPS-MNPs incorporated into the nanofibers when the MNP content was elevated in the precursor. The results also revealed the distribution of MNPs seem to be homogenous in each applied concentration, as shown by remarkable high relative intensity values (red color) of the Raman map, however in the case of 5 w/w% FeTPPS-MNP composition nanoparticles can be found rather in well-defined aggregates, forming less uniform structure inside the PLA fiber structure.

3.3. Biomimetic oxidation of amlodipine catalyzed by FeTPPS-MNP/PLA nanocomposites

Amlodipine (**1**), a dihydropyridine derivative, antihypertensive, Ca channel blocker drug was used as a model substrate in the

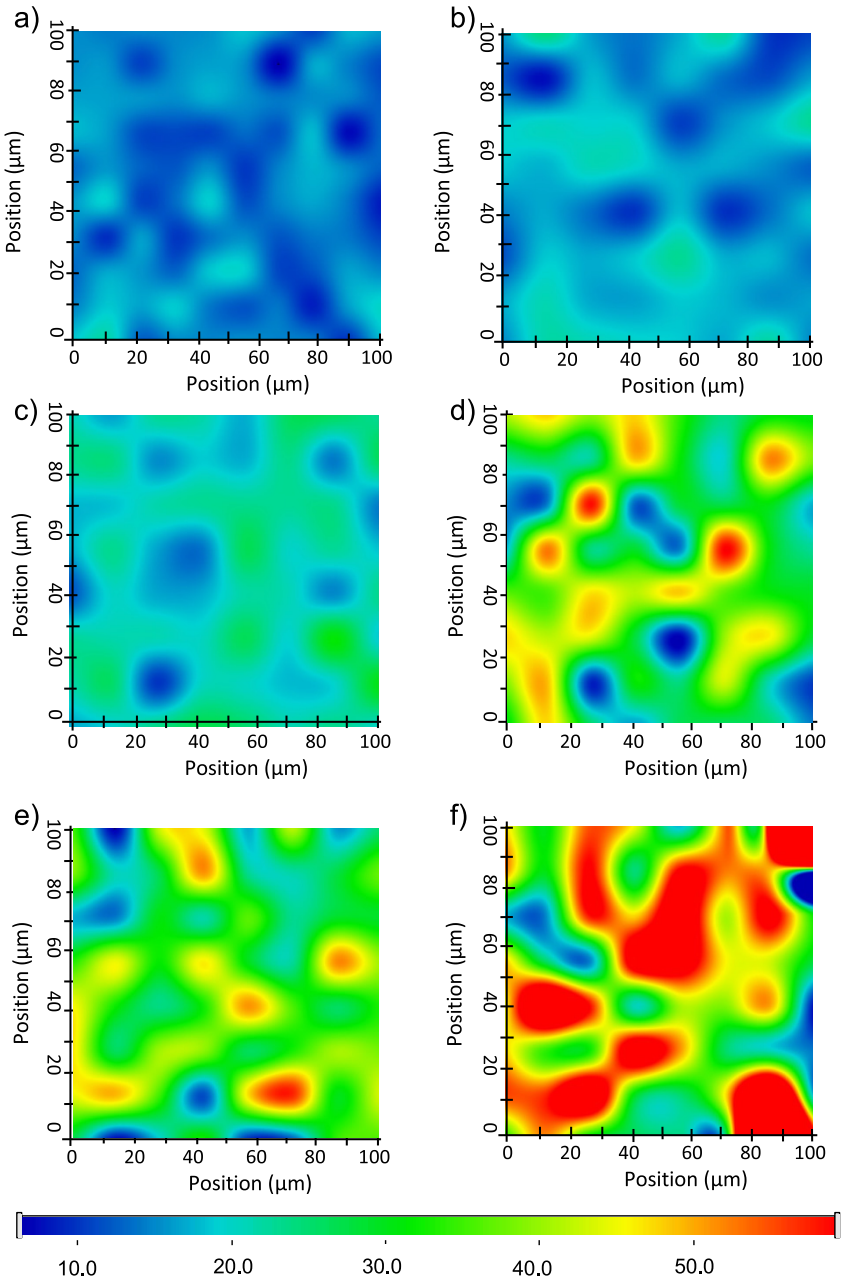

Fig. 4. Raman microscopic analysis of FeTPPS-MNP/PLA composites with different FeTPPS-MNP content of a) – f) 0.16 w/w%, 0.31 w/w%, 0.63 w/w%, 1.25 w/w%, 2.5 w/w%, and 5 w/w%, respectively.

investigation of the biomimetic oxidation catalyzed by the free, by the MNP bound, and by the entrapped MNP/PLA composite system form of metalloporphyrin. The major metabolite of amlodipine in the human body is the pyridine analogue (dehydroamlodipine, **2**), which is formed in a CyP450-catalyzed oxidative transformation. Clinical studies showed that Amlodipine has a quite long elimination of half-life (cc. 35 h) after a single intravenous dose (10 mg) and it is metabolized slowly but extensively by the liver. The first step of amlodipine metabolism is the oxidation of the dihydropyridine moiety to the corresponding pyridine analogue, then oxidative deamination, *O*-dealkylation and oxidative ester hydrolysis is followed by the oxidation of the dihydropyridine moiety in human urine (see in FigureS5). [42,43] In our previous study we showed, that only the major human metabolite, dehydroamlodipine is formed in FeTPPS porphyrin catalyzed (free FeTPPS or immobilized on MNPs) oxidation of amlodipine, thus the model reaction is suitable for mimicking the CyP450 dependent biotransformation. [35].

The catalytic activities of the various FeTPPS-MNP containing PLA composites were investigated in the biomimetic oxidation of amlodipine using *t*-BuOOH as oxygen donor in simple shaken Eppendorf tube reactions in batch mode at 37 °C for 10 min. Fast analysis of reactions was performed by UV–vis spectrophotometry. The conversion and catalytic activity of metalloporphyrin were calculated based on the characteristic absorption spectra of amlodipine and the product, dehydro-amlodipine (see in ESI, FigS3.). Biomimetic (U_B) and specific biomimetic activity (U_P) were calculated (see experimental session). The biomimetic activity U_B increased with increasing FeTPPS-MNP content until 1.25 w/w%. Higher catalyst content led deactivation of the nanocomposite sys-

tem (Fig. 5a). Studying the specific biomimetic activity (U_P) showed that the catalytic activity depended on the metalloporphyrin (FeTPPS) content of the composite system. It can be noted, that U_P continuously decreased due to the increasing FeTPPS-MNP, which might be caused by aggregation in case of high amounts of nanoparticles (Fig. 5b). This might be the reason why the values for FeTPPS-MNP content of 0.63 w/w% and 1.25 w/w% does not differ significantly. Thus, considering U_B and U_P values and the results of fiber fabrication process and structural investigations together, FeTPPS-MNP content at 1.25 w/w% seemed to be the optimal composition. The blank experiment with a fibrous sample containing no FeTPPS-MNP resulted in no product formation.

The comparison of different FeTPPS-based biomimetic catalysts in biomimetic oxidation of amlodipine (**1**) was performed with native FeTPPS (non-immobilized FeTPPS), FeTPPS attached to amino-functionalized MNP (FeTPPS-MNP), FeTPPS-MNP physically mixed with PLA solution (FeTPPS-MNP + PLA), film which was produced from 1.25 w/w% FeTPPS-MNP containing FeTPPS-MNP/PLA precursor (FeTPPS-MNP/PLA film) and nanocomposite produced by electrospinning from 1.25 w/w% FeTPPS-MNP containing FeTPPS-MNP/PLA precursor (FeTPPS-MNP/PLA nanocomposite). Regarding the specific biomimetic activity (U_P), the native FeTPPS, FeTPPS-MNP and FeTPPS-MNP mixed with PLA film were similar, but the presence of PLA enhanced the specific activity of the metalloporphyrin on MNP. Even the metalloporphyrin in solid film forming from FeTPPS-MNP/PLA precursor had much better U_P than either of the first generation FeTPPS-MNP or FeTPPS-PLA systems. An extremely high specific activity of the metalloporphyrin could be achieved with the electrospun FeTPPS-MNP/PLA nanocomposite (Fig. 6). The enhancing effect of solid PLA-based materials – especially in the case of nanostructured PLA – could be attributed to the impact of polymer chains on the orientation of quasi-planar

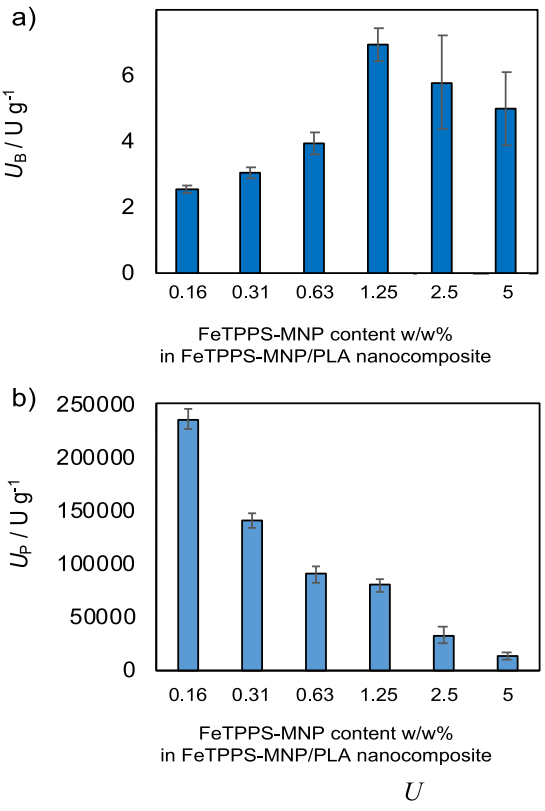

Fig. 5. Effect of FeTPPS-MNP content on the biomimetic activity (U_B) a) and specific biomimetic activity (U_P) b) of FeTPPS-MNP/PLA composites in the biomimetic oxidation of amlodipine (**1**).

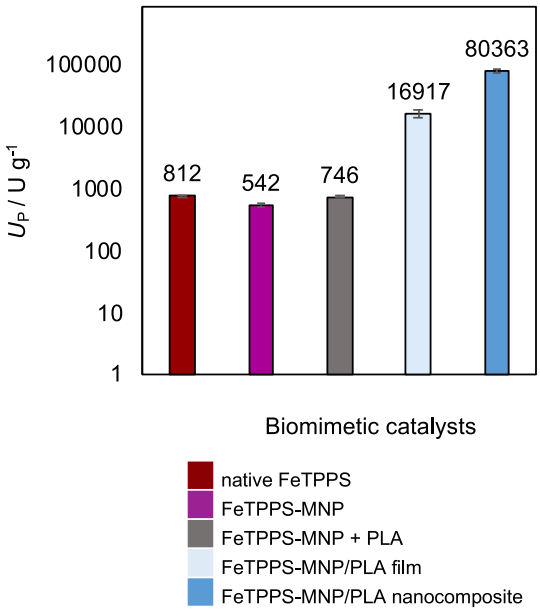

Fig. 6. Specific biomimetic activity (*UP*) of FeTPPS in different catalysts tested by the biomimetic oxidation of amlodipine (**1**).

porphyrin ring resulting in more favorable substrate-catalyst interactions. Accordingly, at the "catalytic site" the FeTPPS and the embedding PLA chains could adopt a three-dimensional arrangement resembling to the active site of CyPs and thus providing favorable conditions of substrate fitting. Worth noting that the so-called catalytic landscape of enzymes is multidimensional and influenced by positive and negative catalytic effects. The "negative catalytic effect" mean exclusion of the unwanted side reactions thus providing protection and stabilization of the forming of „hot intermediate". [44,45] Similar to the protein chains around the active of an enzyme, the polymer chains located around the catalytic sites of the biomimetic composite metalloporphyrin catalyst play the role of negative catalysis leading to enhanced catalytic efficiency. In addition, the PLA chains in their solid forms (film or nanofibrous material) can stabilize a so-called "frozen" dispersion of the catalytic nanoparticles, thus by avoiding aggregation the individual particles retain their accessibility for substrate molecules. Comparing the film and nanostructured composite, it is also remarkable, that much larger specific surface are of nanofibrous composite allowing suitable permeability and diffusion conditions for mass transport supporting the catalytic transformation of substrate.

The reusability of nanocomposite and simple MNP bounded FeTPPS was also investigated in biomimetic oxidation of amlodipine (**1**). Simple washing with the clean solvent of the biomimetic oxidation (methanol and acetate buffer [4:1 V/V, pH = 4.5, 64 mM]) and washing with the solvent, then $NaBH_4$ solution after the first reaction run were compared in the case of FeTPPS-MNP and FeTPPS-MNP/PLA nanocomposite. Regarding the residual specific activity (U_P), it can be seen, that the application of sodium borohydride was a good regenerative agent for both of the catalyst. In addition, MNP/PLA nanocomposite provided a great protective effect, while the residual activity of FeTPPS was around 100 % (Fig. 7.).

In Table 3. comparison of the effectivity of different biomimetic systems is shown, for which conversion value (*c*, %) and turn over number (TON, -) were calculated. Human liver microsomal test (or microsomal stability) of drugs is a gold standard related to vitro pharmacokinetic investigations. [46,47] One of the limitations of

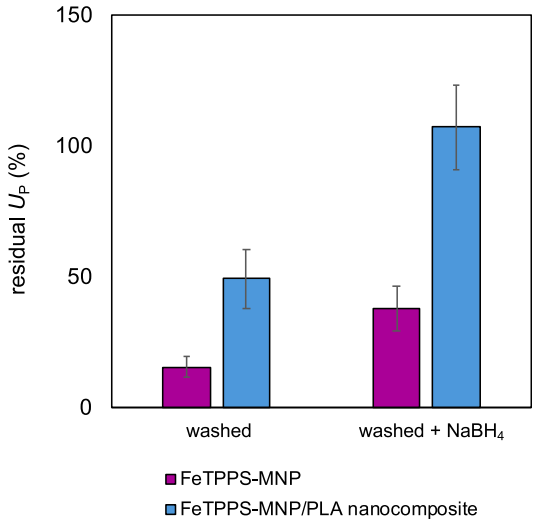

Fig. 7. Effect of washing method (washed: washed with methanol and acetate buffer [4:1 V/V, pH = 4.5, 64 mM] and washed + $NaBH_4$: washed with methanol and acetate buffer [4:1 V/V, pH = 4.5, 64 mM] and $NaBH_4$ solution) on the reusability of immobilized FeTPPS catalyst onto magnetic nanoparticles (MNPs) and into MNP/PLA nanocomposite in biomimetic oxidation of amlodipine (**1**).

Table 3
Comparison of different biomimetic system based on conversion (*c*, %) and turn over number (TON, -) in biomimetic oxidation of amlodipine (**1**).

Biomimetic system	*c* (%)	TON (-)
human liver microsome	2.4 ± 0.1	–
FeTPPS-Silicagel	20.8 ± 12.8	64.8 ± 14.1
FeTPPS-MNP/PLA nanocomposite	24.8 ± 5.1	460.3 ± 33.3

microsome based metabolic investigation can be obviously seen from the really low conversion of amlodipine (**1**). TON for liver microsomal system cannot be calculated while the CyP450 content of these sample is unknown, thus the exact amount of catalytic unit (number of heme prosthetic groups) is hard to determine. Porous silicagels are widely used carrier for batch and continuous-flow catalytic reactions as well, they are also commonly applied for metalloporphyrin immobilization. [10,48,49] Comparing the conversion values of silicagel and nanocomposite-based FeTPPS catalysts it could be concluded that similar conversion was achieved with them, however TON (which considers the metalloporphyrin content of the immobilized catalyst) is an order of magnitude higher in the case of nanocomposite than silicagel carrier.

4. Conclusion

In this study a novel nanocomposite system had been developed, which could be applied for efficient immobilization of biomimetic catalysts such as synthetic metalloporphyrins. This 2nd generation immobilization technique involved a simple ionic binding of FeTPPS as metalloporphyrin onto amino-functionalized magnetic nanoparticles followed by embedding the FeTPPS-covered particles into PLA nanofibers using electrospinning technique. Results showed that the presence of MNPs influenced the fiber deposition process positively. Studies of the biomimetic activity of the immobilized metalloporphyrins on amlodipine (**1**) as model substrate revealed significant effect the catalyst-covered MNP amount within the fibrous composite on the activity. Structural investigation by SEM, SEM-EDAX and Raman microscopy proved that MNPs were successfully entrapped in PLA nanofibers, however the MNP/PLA ratio is important parameter regarding the structural homogeneity of the nanocomposites. The metalloporphyrin within the fibrous FeTPPS-MNP/PLA nanocomposite showed extremely high specific biomimetic activity compared to the FeTPPS-MNP/PLA film or to simple MNP bound FeTPPS systems. Thus, the presented method combining the advantageous properties of magnetic nanoparticles and nanofibers provides a promising way to develop efficient novel catalytic systems. Nanofiber production not only in the laboratory can be performed, but scale up to pilot or industrial level is also achievable. However, it must be noted, that preparation of nanofibrous composite materials requires specific expertise and equipment. Thus, the sustainable production of biomimetic nanocomposites and the quality assurance could cause serious investments in materials and human resources especially at larger scale. As a unique feature, the biomimetic nanocomposites of these type can be integrated into continuous-flow membrane reactors or specific mixer modules used for in vitro metabolism research of early stage of drug discovery with analytical or preparative aims. In addition, this study draws attention to the significant synergistic effect of the proper surface attachment of an enzyme mimicking catalytic agent and embedding the surface attached catalyst into ordered polymeric nanofibrous matrices providing access to new generation biomimetic catalysts with enhanced activity.

CRediT authorship contribution statement

Diána Balogh-Weiser: Conceptualization, Visualization, Resources. **László Poppe:** Writing – review & editing. **Balázs Kenéz:** Investigation, Formal analysis. **Balázs Decsi:** Investigation, Formal analysis. **Gábor Koplányi:** Investigation, Formal analysis. **Gábor Katona:** Formal analysis. **Benjámin Gyarmati:** Formal analysis. **Ferenc Ender:** Methodology. **György T. Balogh:** Methodology, Resources.

Data availability

Data will be made available on request.

Declaration of Competing Interest

The authors declare that they have no known competing financial interests or personal relationships that could have appeared to influence the work reported in this paper.

Acknowledgements

The research reported in this paper and carried out at BME has been supported by the NRDI Fund (TKP2020 NC, Grant No. BME-NC) based on the charter of bolster issued by the NRDI Office under the auspices of the Ministry for Innovation and Technology. D.B.W. acknowledges the János Bolyai Research Scholarship of the Hungarian Academy of Sciences (BO/00175/21), the ÚNKP-21-5 (ÚNKP-21-5-BME-386) New National Excellence Program of the Ministry of Human Capacities and OTKA PD grant (131467) by the NRDI Office. B.D. thanks Servier-Beregi Foundation for the support of this research.

Appendix A. Supplementary material

Supplementary data to this article can be found online at https://doi.org/10.1016/j.molliq.2022.120781.

References

[1] C.F. Samer, K.I. Lorenzini, V. Rollason, Y. Daali, J.A. Desmeules, Applications of CYP450 testing in the clinical setting, Mol. Diagn. Ther. 17 (2013) 165–184, https://doi.org/10.1007/s40291-013-0028-5.

[2] W. Shoombuatong, P. Prathipati, V. Prachayasittikul, N. Schaduangrat, A.A. Malik, R. Pratiwi, S. Wanwimolruk, J.E. Wikberg, M.P. Gleeson, O. Spjuth, C. Nanrasemanat, Towards Predicting the Cytochrome P450 Modulation: From QSAR to Proteochemometric Modeling, Curr. Drug Metab. 18 (2017) 540–555, https://doi.org/10.2174/1389200218666170320121932.

[3] P. Fasinu, P.J. Bouic, B. Rosenkranz, Liver-Based In Vitro Technologies for Drug Biotransformation Studies - A Review, Curr. Drug Metab. 13 (2012) 215–224, https://doi.org/10.2174/138920012798918426.

[4] G. Sowjanya, S. Ganapaty, R. Sharma, In vitro test methods for metabolite identification: A review, Asian J. Pharm. Pharmacol. 5 (5) (2019) 441–450. https://doi.org/10.31024/ajpp.2019.5.3.2.

[5] D. Mansuy, A brief history of the contribution of metalloporphyrin models to cytochrome P450 chemistry and oxidation catalysis, Compt. Rend. Chim. 10 (2007) 392–413, https://doi.org/10.1016/j.crci.2006.11.001.

[6] L.A.D. Zanatta, I. Barbosa, P.B.C. de Sousa Filho, F. Zanardi, L.A.B. Bolzon, O. Serra, Y. Iamamoto, Metalloporphyrins in Drug and Pesticide Catalysis as Powerful Tools to Elucidate Biotransformation Mechanisms, *Mini-Rev*, Org. Chem. 13 (2016) 281–288, https://doi.org/10.2174/1570193X13666160609122754.

[7] M.M.Q. Simões, C.M.B. Neves, S.M.G. Pires, M.G.P.M.S. Neves, J.A.S. Cavaleiro, Mimicking P-450 processes and the use of metalloporphyrins, Pure Appl. Chem. 85 (2013) 1671–1681, https://doi.org/10.1351/PAC-CON-12-11-15.

[8] G. Lente, I. Fábián, Kinetics and mechanism of the oxidation of water soluble porphyrin FeIIITPPS with hydrogen peroxide and the peroxomonosulfate ion, Dalton Trans. (2007) 4268–4275, https://doi.org/10.1039/B708961A.

[9] S. Evans, J.R.L. Smith, The oxidation of ethylbenzene by dioxygen catalysed by supported iron porphyrins derived from iron(III) tetrakis (pentafluorophenyl)porphyrin, J. Chem. Soc., Perkin Trans. 2. (2001), 174–180. https://doi.org/10.1039/B007326L.

[10] T. Fődi, G. Ignácz, B. Decsi, Z. Béni, G.I. Túrós, J. Kupai, D. Balogh-Weiser, I. Greiner, P. Huszthy, G.T. Balogh, Biomimetic Synthesis of Drug Metabolites in Batch and Continuous-Flow Reactors, Chem. Eur. J. 24 (2018) 9385–9392, https://doi.org/10.1002/chem.201800892.

[11] B. Decsi, R. Krammer, K. Hegedűs, F. Ender, B. Gyarmati, A. Szilágyi, R. Tőtős, G. Katona, C. Paizs, G.T. Balogh, L. Poppe, D. Balogh-Weiser, Liver-on-a-Chip-Magnetic Nanoparticle Bound Synthetic Metalloporphyrin-Catalyzed Biomimetic Oxidation of a Drug in a Magnechip Reactor, Micromachines 10 (2019) 668, https://doi.org/10.3390/mi10100668.

[12] S. Nakagaki, F.L. Benedito, F. Wypych, Anionic iron(III) porphyrin immobilized on silanized kaolinite as catalyst for oxidation reactions, J. Mol. Cat. A. 217 (2004) 121–131, https://doi.org/10.1016/j.molcata.2004.03.004.

[13] M. Araghi, F. Bokaei, Manganese(III) porphyrin supported on multi-wall carbon nanotubes: A highly efficient and reusable biomimetic catalyst for oxidative decarboxylation of a-arylcarboxylic acids and oxidation of alkanes with sodium periodate, Polyhedron 53 (2013) 15–19, https://doi.org/10.1016/j.poly.2013.01.052.

[14] S. Nakagaki, C.R. Xavier, A.J. Wosniak, A.S. Mangrich, F. Wypych, M.P. Cantão, I. Denicoló, L.T. Kubota, Synthesis and characterization of zeolite-encapsulated metalloporphyrins, Coll. Surf. A. 168 (2000) 261–276, https://doi.org/10.1016/S0927-7757(99)00503-8.

[15] F. Bedioui, J. Devynck, C. Bied-Charreton, Immobilization of metalloporphyrins in electropolymerized films: design and applications, Acc. Chem. Res. 28 (1995) 30–36, https://doi.org/10.1021/ar00049a005.

[16] M. Halma, K.A.D.d.F. Castro, V. Prévot, C. Forano, F. Wypych, S. Nakagaki, Immobilization of anionic iron(III) porphyrins into ordered macroporous layered double hydroxides and investigation of catalytic activity in oxidation reactions, J. Mol. Cat. A. 310 (1-2) (2009) 42–50.

[17] E.P.S. Tan, C.T. Lim, Mechanical characterization of nanofibers – A review, Comp. Sci. Technol. 66 (2006) 1102–1111, https://doi.org/10.1016/j.compscitech.2005.10.003.

[18] M. Blosi, A.L. Costa, S. Ortelli, F. Belosi, F. Ravegnani, A. Varesano, C. Tonetti, I. Zanoni, C. Vineis, Polyvinyl alcohol/silver electrospun nanofibers: Biocidal filter media capturing virus-size particles, J. Appl. Polym. Sci. 138 (2021) 51380, https://doi.org/10.1002/app.51380.

[19] S. Mohammadzadehmoghadam, Y. Dong, I. Jeffery Davies, Recent progress in electrospun nanofibers: Reinforcement effect and mechanical performance, J. Polym. Sci. Part B. 53 (2015) 1171–1212, https://doi.org/10.1002/polb.23762.

[20] A. Morie, T. Garg, A.K. Goyal, G. Rath, Nanofibers as novel drug carrier – An overview, Artif. Cells Nanomed, Biotechnol. 44 (2016) 135–143, https://doi.org/10.3109/21691401.2014.927879.

[21] S.F. Anis, A. Khalil, Saepurahman, G. Singaravel, R. Hashaikeh, A review on the fabrication of zeolite and mesoporous inorganic nanofibers formation for catalytic applications, Micropor. Mesopor. Mat. 236 (2016) 176–192.

[22] G. Koplányi, E. Sánta-Bell, Z. Molnár, G.D. Tóth, M. Józó, A. Szilágyi, F. Ender, B. Pukánszky, B.G. Vértessy, L. Poppe, D. Balogh-Weiser, Entrapment of Phenylalanine Ammonia-Lyase in Nanofibrous Polylactic Acid Matrices by Emulsion Electrospinning, Catalysts 11 (2021) 1149, https://doi.org/10.3390/catal11101149.

[23] M.S. Peresin, Y. Habibi, J.O. Zoppe, J.J. Pawlak, O.J. Rojas, Nanofiber composites of polyvinyl alcohol and cellulose nanocrystals: manufacture and characterization, Biomacromolecules 11 (2010) 674–681, https://doi.org/10.1021/bm901254n.

[24] S. Virji, J.D. Fowler, C.O. Baker, J. Huang, R.B. Kaner, B.H. Weiller, Polyaniline nanofiber composites with metal salts: Chemical sensors for hydrogen sulfide, Small 1 (2005) 624–627, https://doi.org/10.1002/smll.200400155.

[25] W.C. Huang, W. Wang, C. Xue, X. Mao, X. Effective Enzyme Immobilization onto a Magnetic Chitin Nanofiber Composite, ACS Sus. Chem. Eng. 6 (2018) 8118–8124. https://doi.org/10.1021/acssuschemeng.8b01150.

[26] A. Celebioglu, F. Topuz, T. Uyar, Facile and green synthesis of palladium nanoparticles loaded into cyclodextrin nanofibers and their catalytic application in nitroarene hydrogenation, New J. Chem. 43 (2019) 3146–3152, https://doi.org/10.1039/C8NJ05133J.

[27] Z. Li, C. Wang, Electrospinning Technique and Unique Nanofibers in SpringerBriefs in Materials Li, Z., Wang (Eds.), Springer: Berlin, Heidelberg, Germany, 2013, https://doi.org/10.1007/978-3-642-36427-3.

[28] P. Modhisa, T. Nyokong, Fabrication of phthalocyanine-magnetic nanoparticles hybrid nanofibers for degradation of Orange-G, J. Mol. Cat. A. 381 (2014) 132–137, https://doi.org/10.1016/j.molcata.2013.10.012.

[29] S. Galland, R.L. Andersson, M. Salajkova, V. Ström, R.T. Olsson, L.A. Berglund, Cellulose nanofibers decorated with magnetic nanoparticles – synthesis, structure and use in magnetized high toughness membranes for a prototype loudspeaker, J. Mater. Chem. C. 1 (2013) 7963–7972, https://doi.org/10.1039/C3TC31748J.

[30] H. Hu, W. Jiang, F. Lang, X. Zeng, S. Ma, Y. Wu, Z. Gu, Synergic effect of magnetic nanoparticles on the electrospun aligned superparamagnetic nanofibers as a potential tissue engineering scaffold, RSC Adv. 3 (2013) 879–886, https://doi.org/10.1039/C2RA22726F.

[31] N. Amiralian, M. Mustapic, M.S.A. Hossain, C. Wang, M. Konarova, J. Tang, J. Na, A. Khan, A. Rowan, Magnetic nanocellulose: A potential material for removal of dye from water, J. Hazard. Mater. 394 (2020), https://doi.org/10.1016/j.jhazmat.2020.122571.

[32] A. Jedlovszky-Hajdu, K. Molnar, P.M. Nagy, K. Sinko, M. Zrinyi, Preparation and properties of a magnetic field responsive three-dimensional electrospun polymer scaffold, Coll. Surf. A. 503 (2016) 79–87, https://doi.org/10.1016/j.colsurfa.2016.05.036.

[33] H.J. Harossh, Y. Dong, G.D. Ingram, Synthesis, Morphological Structures, and Material Characterization of Electrospun PLA:PCL/Magnetic Nanoparticle Composites for Drug Delivery, Poly. Phys. 51 (2013) 1607–1617, https://doi.org/10.1002/polb.23374.

[34] R. Contreras-Caceres, L. Cabeza, G. Perazzoli, A. Diaz, J.M. Lopez-Romero, C. Melguizo, J. Prados, Electrospun Nanofibers: Recent Applications in Drug Delivery and Cancer Therapy, Nanomaterials 9 (2019) 9, 656. https://doi.org/10.3390/nano9040656.

[35] D. Balogh-Weiser, B. Decsi, R. Krammer, G. Dargó, F. Ender, J. Mizsei, R. Berkecz, B. Gyarmati, A. Szilágyi, R. Tőtős, C. Paizs, L. Poppe, G.T. Balogh, Magnetic Nanoparticles with Dual Surface Functions—Efficient Carriers for Metalloporphyrin-Catalyzed Drug Metabolite Synthesis in Batch and Continuous-Flow Reactors, Nanomaterials 10 (2020) 2329, https://doi.org/10.3390/nano10122329.

[36] D. Weiser, L.C. Bencze, G. Bánóczi, F. Ender, R. Kiss, E. Kókai, A. Szilágyi, B.G. Vértessy, Ö. Farkas, C. Paizs, L. Poppe, Phenylalanine Ammonia-Lyase-Catalyzed Deamination of an Acyclic Amino Acid: Enzyme Mechanistic Studies Aided by a Novel Microreactor Filled with Magnetic Nanoparticles, ChemBioChem 16 (2015) 2383–12288, https://doi.org/10.1002/cbic.201500444.

[37] A.O. Imarah, P. Csuka, N. Bataa, B. Decsi, E. Sánta-Bell, Z. Molnár, D. Balogh-Weiser, L. Poppe, Magnetically Agitated Nanoparticle-Based Batch Reactors for Biocatalysis with Immobilized Aspartate Ammonia-Lyase, Catalysts 11 (2021) 483, https://doi.org/10.3390/catal11040483.

[38] F. Nagy, G. Tasnádi, D. Balogh-Weiser, E. Bell, M. Hall, K. Faber, L. Poppe, Smart Nanoparticles for Selective Immobilization of Acid Phosphatases, ChemCatChem 10 (2018) 3490–3499, https://doi.org/10.1002/cctc.201800405.

[39] F. Nagy, E. Sánta-Bell, M. Jipa, G. Hornyánszky, A. Szilágyi, K. László, G. Katona, C. Paizs, L. Poppe, D. Balogh-Weiser, Cross-Linked Enzyme-Adhered Nanoparticles (CLEANs) for Continuous-Flow Bioproduction, ChemSusChem 15 (2022) e202102284.

[40] Y.S. Li, J.S. Church, A.L. Woodhead, Infrared and Raman spectroscopic studies on iron oxide magnetic nano-particles and their surface modifications, J. Magn. Mag. Mater. 324 (2012) 1543–1550, https://doi.org/10.1016/j.jmmm.2011.11.065.

[41] Y.P. Yew, K. Shameli, M. Miyake, N.B.B. Ahmad Khairudin, S.E.B. Mohamad, H. Hara, M.F.B. Mad Nordin, K.X. Lee, An Eco-Friendly Means of Biosynthesis of Superparamagnetic Magnetite Nanoparticles via Marine Polymer, IEEE Trans. Nanotechnol. 16 (6) (2017) 1047–1052.

[42] Y. Zhu, F. Wang, Q. Li, M. Zhu, A. Du, W. Tang, W. Chen, Amlodipine metabolism in human liver microsomes and roles of CYP3A4/5 in the dihydropyridine dehydrogenation, Drug Metab. Dispos. 42 (2) (2014) 245–249.

[43] M. Gerisch, R. Heinig, A. Engelen, D. Lang, P. Kolkhof, M. Radtke, J. Platzek, K. Lovis, G. Rohde, T. Schwarz, Biotransformation of Finerenone, a Novel Nonsteroidal Mineralocorticoid Receptor Antagonist, in Dogs, Rats, and Humans, In Vivo and In Vitro, Drug Metab. Dispos. 46 (2018) 1546–1555, https://doi.org/10.1124/dmd.118.083337.

[44] J. Rétey, Enzymic Reaction Selectivity by Negative Catalysis or How Do Enzymes Deal with Highly Reactive Intermediates?, Angew Chem. 29 (1990) 355–361, https://doi.org/10.1002/anie.199003551.

[45] B. Vögeli, T.J. Erb, 'Negative' and 'positive catalysis': complementary principles that shape the catalytic landscape of enzymes, Curr. Opinn. Chem. Biol. 47 (2018) 94–100, https://doi.org/10.1016/j.cbpa.2018.09.013.
[46] K.M. Knights, D.M. Stresszer, J.O. Miners, C.L. Crespi, In Vitro Drug Metabolism Using Liver Microsomes, Curr. Prot. Pharmacol. (2016) 7.8.1–7.8.24. https://doi.org/10.1002/cpph.9.
[47] S. Asha, M. Vidyavathi, Role of Human Liver Microsomes in In Vitro Metabolism of Drugs—A Review, App. Biochem. Biotech. 160 (2010) 1699–1722, https://doi.org/10.1007/s12010-009-8689-6.
[48] M. Ghiaci, F. Molaie, M.E. Sedaghat, N. Doroskar, Metalloporphyrin covalently bound to silica. Preparation, characterization and catalytic activity in oxidation of ethyl benzene, Cat. Com. 11 (2010) 694–699, https://doi.org/10.1016/j.catcom.2010.01.023.
[49] F.L. Benedito, S. Nakagaki, A.A. Sack, P.G. Perlata-Zamora, C.M.M. Costa, Study of metalloporphyrin covalently bound to silica as catalyst in the ortho-dianisidine oxidation, Appl. Catal. A. 250 (2003) 1–11, https://doi.org/10.1016/S0926-860X(02)00663-4.